Geophysical Research Letters

RESEARCH LETTER
10.1029/2019GL084601

Disentangling Dynamic Contributions to Summer 2018 Anomalous Weather Over Europe

Marie Drouard[1], **Kai Kornhuber**[1,2,3], **and Tim Woollings**[1]

[1]Atmospheric, Oceanic and Planetary Physics, University of Oxford, Oxford, UK, [2]National Centre for Atmospheric Science, UK, [3]Earth Institute, Columbia University, New York, NY, USA

Key Points:
- Record high NAO+ and a stationary Wave-7 pattern both played a role in summer 2018 heat and high-precipitation events over Europe
- Quantification of their contributions to the observed anomalies is performed using linear regressions
- Anomalies of +2–2.5 C over France and the United Kingdom are explained by their concurrent occurrence from 21 June to 14 July

Supporting Information:
- Supporting Information S1

Correspondence to:
M. Drouard,
marie.drouard@physics.ox.ac.uk

Citation:
Drouard, M., Kornhuber, K., & Woollings, T. (2019). Disentangling dynamic contributions to summer 2018 anomalous weather over Europe. *Geophysical Research Letters*, *46*, 12,537–12,546. https://doi.org/10.1029/2019GL084601

Received 17 JUL 2019
Accepted 13 OCT 2019
Accepted article online 29 OCT 2019
Published online 7 NOV 2019

Abstract Summer 2018 was one of the driest and hottest experienced over northwestern Europe. In contrast, over southern Europe, it was marked by cooler and wetter conditions with flooding over Greece and Spain. This contrasting pattern was particularly enhanced over a 3-week period starting on 21 June. Two atmospheric patterns are thought to have largely contributed to this anomalous weather: the positive North Atlantic Oscillation (NAO+) and a Wave-7 pattern. Using linear regressions on detrended data, we show that the NAO+ was mainly responsible for the observed seasonal anomalies. However, during the 3-week period, the rare combination of the NAO+ and Wave-7 is necessary to explain the pattern of the observed anomalies. The global warming trend and, to a lesser extent, nonlinear processes are shown to have furthermore strongly modulated the anomalies associated with these two patterns.

1. Introduction

June-July-August (JJA) 2018 was marked by anomalous weather conditions with several heat and flooding events occurring simultaneously over the Northern Hemisphere (NOAA, 2018). Over northwestern Europe, clear-sky conditions, high temperature, and low precipitation dominated the whole summer (Met Office, 2018; Météo France, 2018), whereas lower temperatures and higher precipitation were recorded over Greece and northern Spain. These contrasting seasonal weather conditions were particularly enhanced over a 3-week period from late June to mid-July (Kornhuber et al., 2019).

Previous studies suggested two different drivers to explain these simultaneous heat and high-precipitation events observed in the Northern Hemisphere. Kornhuber et al. (2019) argued that the late June to mid-July concomitant heat waves and flooding were due to an exceptionally strong stationary Rossby Wave-7 pattern. The World Weather Attribution Project (2018, hereafter WWAP) and Vogel et al. (2019) focused on the role of anthropogenic climate change in the occurrence of the 2018 heat events. According to the WWAP, the probability of occurrence of the June–July 2018 heat events doubled due to anthropogenic climate change. Vogel et al. (2019) later stated that it was *virtually certain* that the 2018 large-scale heat events would not have occurred without anthropogenic climate change.

However, these studies do not explain the persistence over the whole summer of warmer and drier conditions over northwestern Europe and cooler and wetter conditions over southern Europe. Here, we focus on the North Atlantic European (NAE) region to analyze the broader circulation patterns responsible for the observed anomalies. The contributions of two patterns are investigated: the summer North Atlantic Oscillation (NAO), which is well known as a dominant pattern in the NAE region and which reflects jet and storm track variability (Bladé et al., 2012; Dong et al., 2013; Feldstein, 2007; Folland et al., 2009; Hurrell et al., 2003) and the stationary Rossby Wave-7 pattern identified by Kornhuber et al. (2019) as a recurrent pattern, which was particularly active in June–July 2018. We aim to quantify the fraction of the anomalous weather in this season attributable to these two patterns alone and not to do a full dynamics/thermodynamics comparison. Two periods of time were analyzed, a 3-week period starting on 21 June (when the Wave-7 was particularly strong) and the JJA season, to describe the impact of these patterns at different timescales. Data and methods are introduced in section 2. Results are presented in sections 3 and 4 and discussed in section 5.

2. Data and Methods

Our analysis is based on daily 300-hPa geopotential height (Z300), sea level pressure (SLP), 300-hPa meridional wind (V300), 2-m temperature and precipitation rate, and 6-hourly surface temperature from the

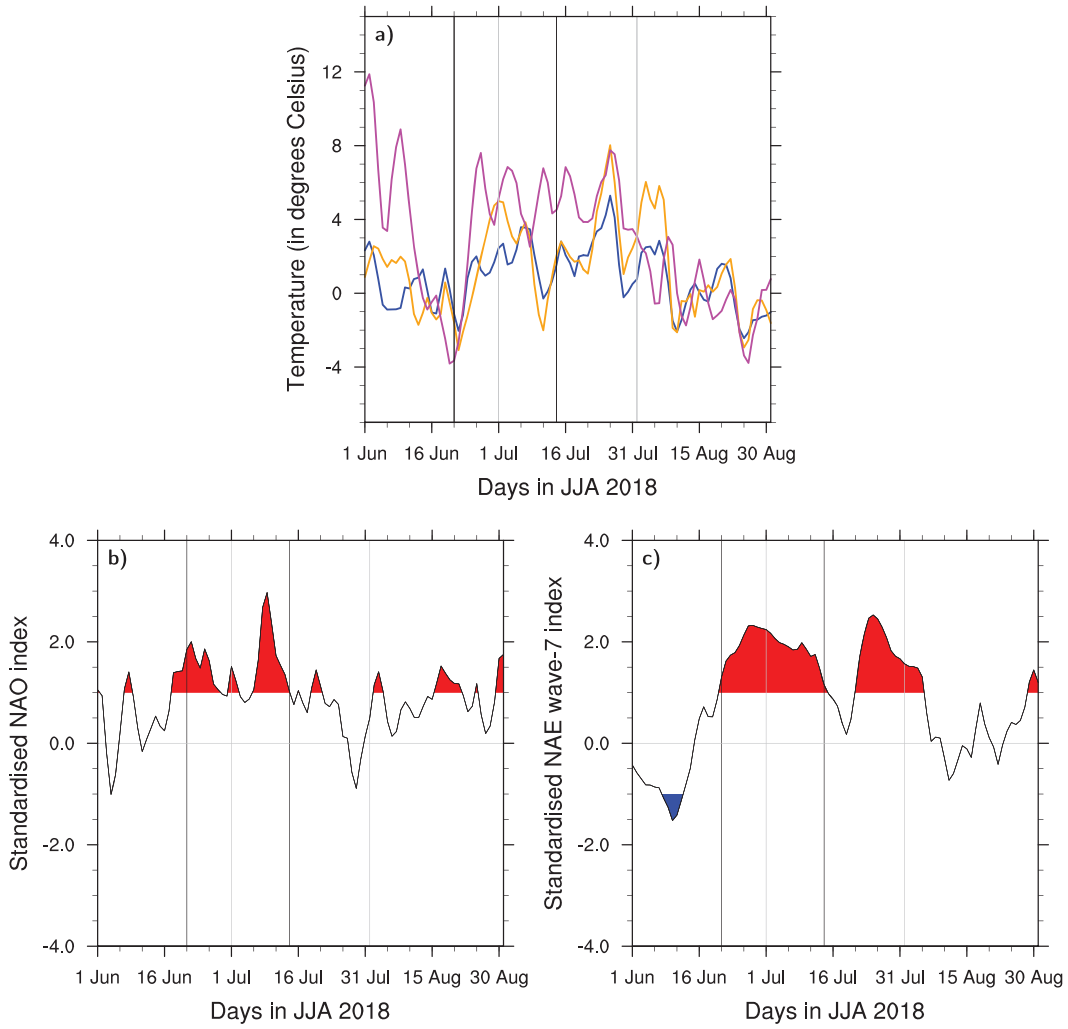

Figure 1. (a) National Centers for Environmental Prediction/National Center for Atmospheric Research Reanalysis 1 three-day-mean noon surface temperature anomaly (annual cycle removed) in London (blue line), Paris (orange line), and Oslo (magenta line) in JJA 2018. (b) Standardized NAO index in JJA 2018. Red areas show where the index is greater or equal to one standard deviation and blue areas where it is smaller or equal to minus one standard deviation. (c) Same as (b) but for the standardized Wave-7 index. Gray vertical lines show 1 July and 1 August. Black vertical lines show 21 June and 14 July. NAO = North Atlantic Oscillation; JJA = June-July-August.

National Centers for Environmental Prediction/National Center for Atmospheric Research Reanalysis 1 (Kalnay et al., 1996). All the data are on a 2.5° × 2.5° grid except for the precipitation rate, which is on a 1.91° × 1.875° grid. Daily anomalies are computed relative to the daily JJA 1979–2018 climatology, which is smoothed using a 5-day running mean. Seasonal anomalies are computed relative to the seasonal JJA 1979–2018 climatology. All the data are detrended except for the surface temperature shown in Figure 1a and anomalies in Figures 2a, 2e, 3a, 3e, 4a, and 4e. The trend is linearly computed using 1979–2018 daily data at each grid point.

2.1. Summer NAO Index

The daily summer NAO is defined as the first empirical orthogonal function (EOF) of the SLP over the North Atlantic (20–80°N, 90°W to 40°E; see index in Figure 1b). The seasonal summer NAO is similarly defined as the first EOF of the seasonal JJA mean SLP over the North Atlantic. The SLP has been weighted by the square root of the cosine of the latitude for the EOF calculation.

2.2. Summer NAE Wave-7 Index

Motivated by the events of summer 2018, Kornhuber et al. (2019) calculated a composite high-amplitude Wave-7 pattern (see their Figure 3b). This is derived by Fourier decomposing weekly mean V300

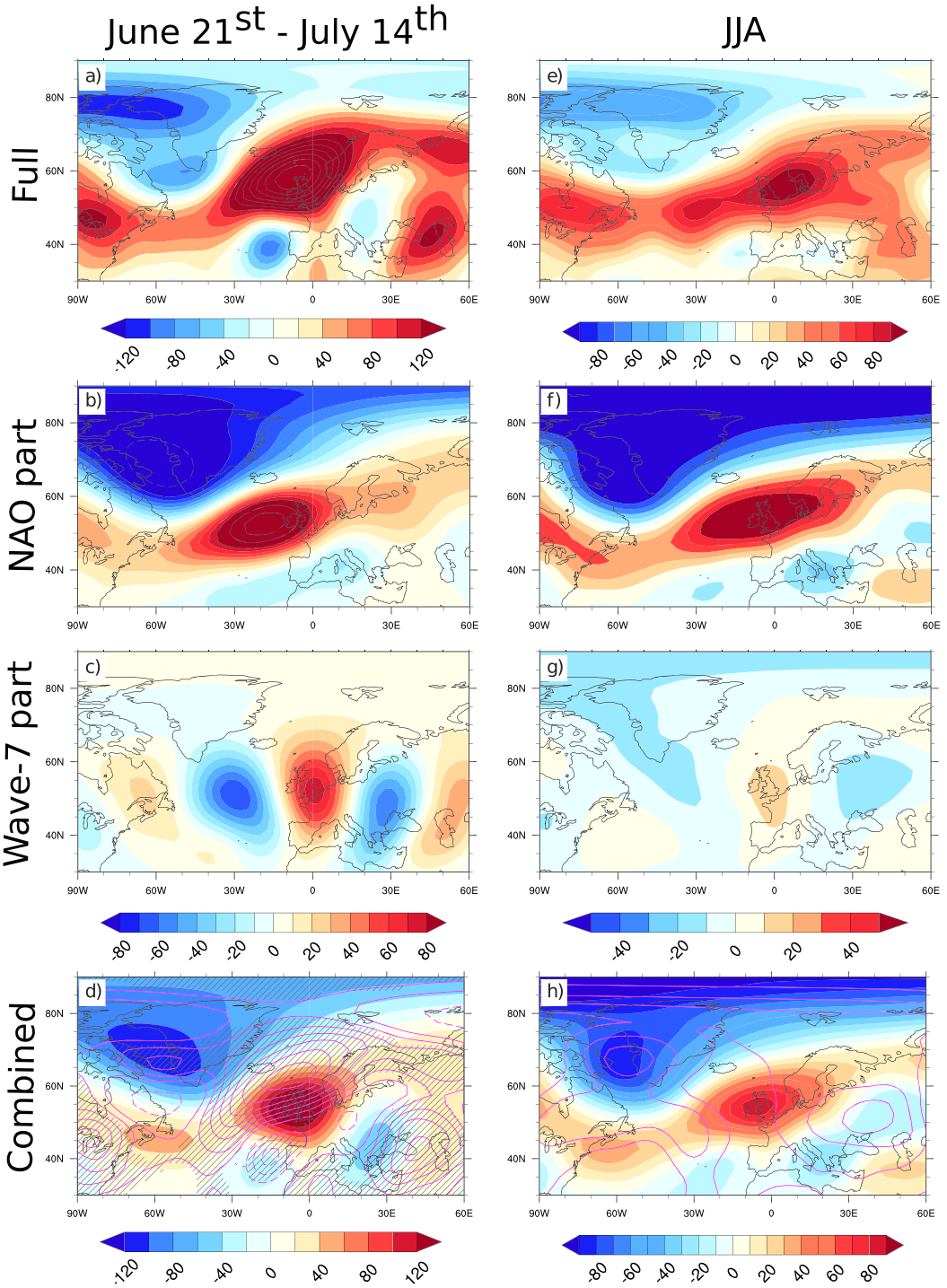

Figure 2. (a) Full Z300 anomaly averaged between 21 June and 14 July 2018 (shadings and contours in square meters per square second). First contour is 120 m^2/s^2, interval: 20 m^2/s^2. (b) NAO contribution to the Z300 anomaly averaged over the same period (shadings and contours in square meters per square second; see color bar below panel (c). First contour is 80 m^2/s^2, interval: 10 m^2/s^2). (c) Same as (b) but for the Wave-7 (m^2/s^2). (d) Sum of the NAO and Wave-7 pattern contributions averaged over the same period (shadings in square meters per square second). Magenta contours show the difference between the full anomaly (shown in panel a) and the sum of two contributions (shown in shading). Solid contours show positive values and dashed contours negative values, with interval: 20 m^2/s^2. (e–h) Same analyses as in (a)–(d) but for the whole JJA 2018 (computed with seasonal values). Hatched areas in Figure 2d indicate that the difference is statistically significant using a two-sample *t* test with a 10% threshold. The significance test cannot be performed on a single season of data, explaining why no hatchings are visible in Figure 2h. NAO = North Atlantic Oscillation; JJA = June-July-August.

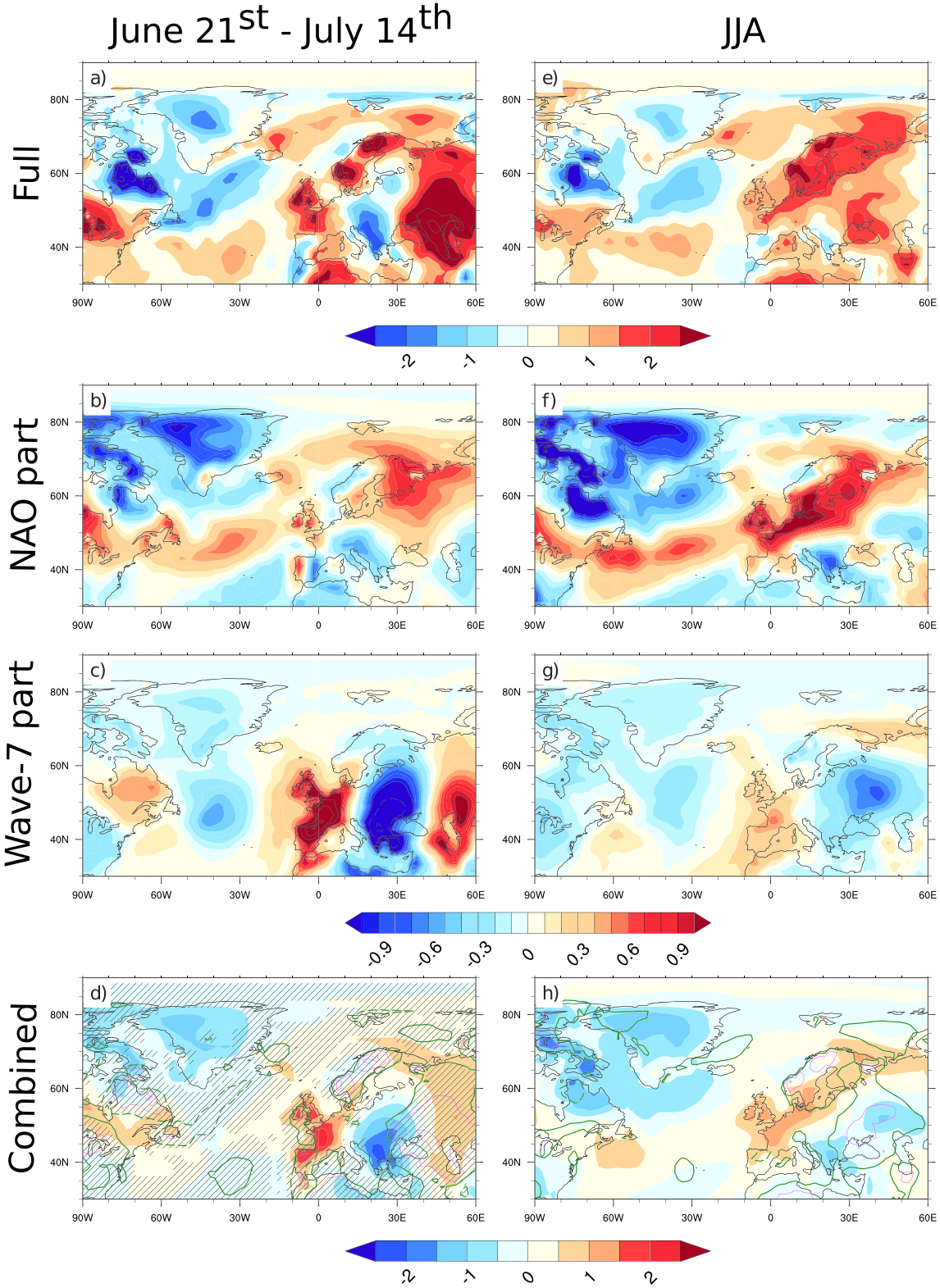

Figure 3. Same as Figure 2 but for the 2-m temperature (°C). (a and e) Black contours are every 1° starting at 2.5° for the positive values and −2.5° for the negative values. Solid contours show positive values and dashed contours negative values. (c and f) Black contours are every 0.4° starting at 1.0° for the positive values and −1.0° for the negative values. (d and h) Magenta contours are every 2 °C starting at 0 °C. Thick solid and dashed green contours indicate the 1 and −1 °C contour line, respectively. NAO = North Atlantic Oscillation; JJA = June-July-August.

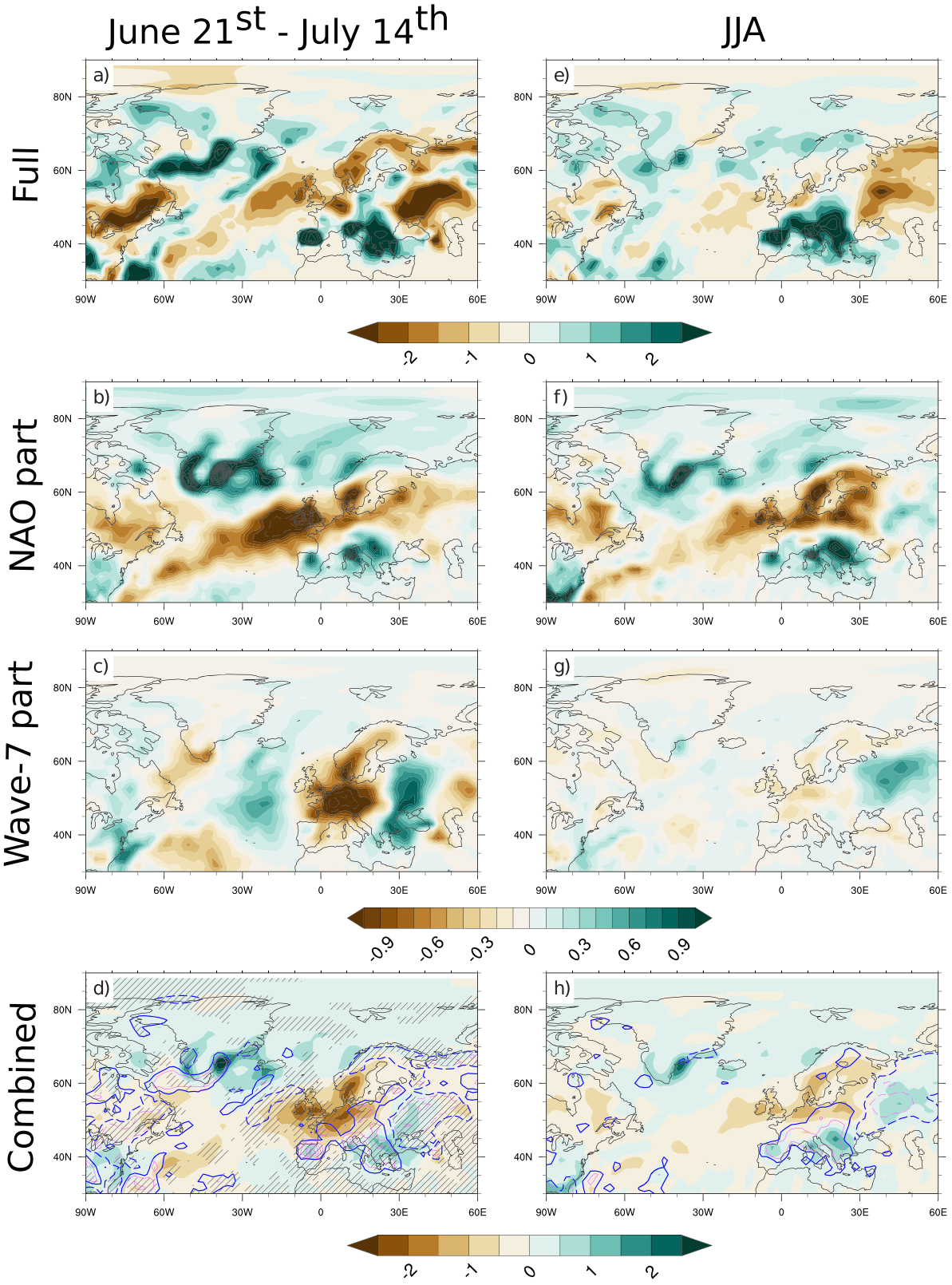

Figure 4. Same as Figure 3 but for the daily precipitation (mm/day). (b, c, and f) Black contours are every 0.2 mm/day starting at 1 mm/day for the positive values and −1 mm/day for the negative values. (d and h) Magenta contours are every 2 mm/day starting at 0. Thick solid and dashed blue contours indicate the 1- and −1-mm/day contour line, respectively. NAO = North Atlantic Oscillation; JJA = June-July-August.

(see Kornhuber et al. 2019). Here we derive a daily Wave-7 index based on the spatial Spearman correlation of the V300 (smoothed prior to computation using a 7-day running mean) with this high-amplitude Wave-7 event composite over the midlatitudes of the Euro-Atlantic sector (37.5–57.5°N, 30°W to 60°E; see index for summer 2018 in Figure 1c). The seasonal NAE Wave-7 index is built similarly but using the seasonal-mean V300.

2.3. Contribution Computations Using Linear Regressions

To estimate the contributions of the NAO and Wave-7 to the atmospheric circulation, the Z300, 2-m temperature and precipitation were linearly regressed on both indices to get the regression coefficient and *y* intercept. This allows us to compute the linear NAO and Wave-7 contributions to the atmospheric circulation for both periods.

3. NAO and Wave-7 Impacts

3.1. Early Period: 21 June to 14 July

From 21–25 June, northwestern European surface temperatures increased by 4 to 12 °C and remained 2 to 5 °C above average for about 20 days in London, Paris, and Olso (Figure 1a). Concurrent strong positive Z300 anomalies were observed over northwestern Europe—that locally extended over southeastern Spain and France—and western Russia (Figure 2a). These were flanked by negative anomalies over Baffin Bay/Greenland, west of Portugal, and over Italy/Greece. The positive Z300 anomalies were associated with warmer and drier conditions (+0.5–4.5 °C with a precipitation deficit of −0.5–2.5 mm/day; Figures 3a and 4a), while the negative Z300 anomalies were associated with cooler and wetter weather (e.g., −2 °C and +2 mm/day over Greece and +8 mm/day over northern Spain).

Warmer and drier weather over northwestern Europe with simultaneous cooler and wetter conditions over southern Europe are distinctive features of the positive summer NAO (NAO+; Bladé et al., 2012; Folland et al., 2009). Figure 1b shows that the NAO was strongly positive and reached a record high value of 2.97 on 9 July 2018. Figures 2b, 3b, and 4b show the part of the respective anomalies that can be attributed to the NAO using the linear regression approach. The NAO explains the northwest-southeast tripole observed in the Z300, temperature, and precipitation. However, it does not explain (1) the meridional component of the anomalies (southward extension of the positive Z300 anomaly over southeastern Spain, France, and Germany), (2) the strong anomalies over western Russia, and (3) the full amplitude of the anomalies.

The meridional extension in the observed anomalies (Figures 2a, 3a, and 4a) can be attributed to the particularly strong NAE Wave-7 pattern identified by Kornhuber et al. (2019; Figure 1c). Indeed, it is associated with meridionally elongated negative Z300 anomalies over eastern Europe, flanked to the west and east by positive anomalies (Figure 2c). This results in warmer and drier conditions over western Europe and western Russia and cooler and wetter conditions over eastern Europe (Figures 3c and 4c). The temperature and precipitation anomalies associated with this pattern are stronger than those due to the NAO (compare Figures 3b and 4b with Figures 3c and 4c).

Summing the NAO and Wave-7 contributions strengthens the Z300, temperature, and precipitation anomalies over western Eurasia (shadings in Figures 2d, 3d, and 4d). Over Brittany, they explain 20% to 60% of the observed temperature anomalies and over the United Kingdom, northern and western France, and Belgium it increases to 50% to 110% (up to +2.5 °C; Figure 3d). Ten to twenty percent (+0.5 mm/day) of the precipitation anomalies over Greece are explained by these two patterns (Figure 4d). The difference with the observed anomalies is not significant over large parts of western and central Europe for the Z300 and temperature and over parts of France, Germany, and Finland for the precipitation. There, these two atmospheric patterns explain most of the observed weather.

Elsewhere the difference with the observed anomalies is significant. This is particularly striking over western Iberia, western Scandinavia, and eastern Ukraine, where the observed anomalies are opposite to the reconstructed ones (Figure 3d). These discrepancies could arise from (1) limitations in the linear regression model as it does not take into account nonlinear relationships or variations in the pattern (e.g., the use of fixed NAO and Wave-7 patterns explains the weaker Z300 reconstructed anomaly west of Portugal [Figure 2d] that is responsible for the temperature discrepancy over western Iberia); (2) nonstationarity in the NAO pattern (Baker et al., 2019; Bladé et al., 2012); and (3) trends in the observed anomalies as the data used for the linear regressions are detrended (section 4). As shown later, trends in the data explain large

part of the discrepancies observed over Scandinavia and eastern Ukraine (section 4); (4) other circulation patterns or other more local phenomena.

Thus, while the Wave-7 explains the simultaneous heat and precipitation events over large parts of the Northern Hemisphere (Kornhuber et al., 2019), it is not sufficient to explain the pattern of the more local anomalies observed over the NAE region. There, the summer NAO+ also played an important role and the combination of these two recurrent circulation patterns is necessary to understand the early period weather. The NAO+ and Wave-7 indices are statistically independent in the reanalysis and do no exhibit any lead-lag relationships (Figure S1 in the supporting information). The simultaneous occurrence of large anomalies in both is hence rare. Finally, these two patterns show strong values over other periods of JJA 2018, though not simultaneously. In the following, we will focus on their impacts on JJA 2018 seasonal means.

3.2. JJA 2018

JJA 2018 was marked by a record high and persistent NAO+ (Figure S2): The NAO index was greater or equal to 1 for more than a third of the season and lower or equal to −1 for only 1 day. Only three other years since 1979 show large (but smaller) ratio of NAO+ over NAO− days. This led to a strongly positive seasonal value of 2.17 in JJA 2018, the strongest over the considered period (not shown). The daily NAO was the highest over the early period, but its index remained positive over most of the summer, albeit slightly weaker.

The NAE Wave-7 pattern was strongly positive during two periods: 21 June to 14 July and 21 July to 7 August. Over the rest of the summer, this pattern was weak or negative.

The northwest-southeast tripole of the NAO+ is clearly seen in the JJA 2018 seasonal Z300 anomaly (Figures 2e and 2f). So, despite weaker positive values outside of the previously studied period, the NAO+ imprint on the seasonal atmospheric circulation was very strong. On the contrary, despite the two periods of high NAE Wave-7 index, the Wave-7 contribution to the JJA 2018 seasonal-mean Z300 anomaly barely stands out in Figure 2g.

Again, the NAO+ dipole is clearly seen in the observed 2-m temperature anomalies (Figures 3e and 3f). The seasonal NAO+ temperature anomalies over northwestern Europe are even stronger and more spatially extended than during the early period (Figures 3b and 3f), emphasizing the stronger NAO+ contribution at the seasonal timescale. Despite the weak circulation signal, the Wave-7 does have an impact on seasonal-mean temperatures and contributes up to +0.3–0.5 °C to the positive anomaly seen over western Europe (Figure 3g).

A northwest-southeast tripole over Europe and negative anomalies over western Russia are visible in the seasonal precipitation anomalies (Figure 4e). This tripole is similar to the precipitation NAO+, but with a much less extended and weaker positive anomaly and a stronger and more extended negative anomaly to the south (Figure 4f). The Wave-7 contribution is again weak (values smaller than ±0.2 mm/day; Figure 4g). Again, most of the signal comes from the NAO+ despite slight differences in amplitude and pattern.

Despite a strong NAO+ imprint, differences to the observed fields are still visible. For the Z300, these are smaller than during the early period and are characterized by a general Z300 increase, which is particularly strong over Ukraine/western Russia and the Baffin Bay (Figure 2h). This is associated with a +1 °C difference (locally up to +2 °C) over Ukraine/Russia (Figure 3h). Over the rest of Europe, the difference is smaller than 1 °C, to the exception of Scandinavia where it reaches values of +2 °C. The difference to the observed precipitation is distinct and is mostly related to differences in the observed and NAO+ precipitation tripoles shown previously (Figure 4h).

Thus, the NAO+ clearly dominated the atmospheric circulation of JJA 2018 and strongly impacted weather over western Eurasia. At this timescale, the Wave-7 had a much weaker impact on the observed anomalies. Differences between these two patterns and the observed anomalies are also seen at the seasonal scale, albeit weaker than for the early period. They partly arise from trends in the data as shown in the following section.

4. Contribution of Trends

Strong trends have been previously evidenced in various fields in summer over Europe (van Oldenborgh et al., 2009), implying that a large part of the difference with the observed anomalies might come from these. Figures S3 and S4 show the linear trend contribution to the observed anomalies and the difference between the observed anomalies and the combined contributions of the NAO+, Wave-7 and trend.

The trend contribution to summer 2018 Z300 anomalies consists of a tripole with a negative anomaly over the North Atlantic flanked by positive anomalies to the northwest and southeast (Figure S3b). Its weight on the early period anomalies is weaker than on the seasonal anomalies. Indeed, adding the trend does not decrease the difference from observations for the early period (Figure S4a), but it does for JJA 2018 (Figure S4d). However, at both timescales, adding the trend contribution strengthens some differences (e.g., stronger negative anomalies west of Portugal and over Germany for the early period or over the North Atlantic for JJA 2018).

The warming-trend contribution to the 2-m temperature anomalies over western Eurasia consists of positive values ranging from +0.2 (Wales) to +2.6 °C (northern Scandinavia; Figure S3c). Over Scandinavia and western Russia, adding the warming-trend contribution completely offsets the negative temperature anomaly seen in Figures 3d and 3h (Figures S4b and S4e). Therefore, at both timescales, the warming trend reverses the negative temperature anomalies that would have been expected over Norway and western Russia in response to the combined NAO+ and Wave-7. This confirms the ability of warming trends to locally reverse the impacts of a given circulation pattern as previously shown (e.g., for winter 2009/2010; Cattiaux et al., 2010).

Nevertheless, over southern Norway, adding the trend does not reduce the difference seen in Figures 3d and 3h. The residual could be due to nonlinearity associated with mountain snow melt. Over western Russia, for the early period, +1 °C and locally up to +2 °C are still left unexplained, implying that another circulation pattern or local soil-moisture feedback processes (Fischer, 2014; Miralles et al., 2014) could play a role there. And at the seasonal timescale, the small residual difference could be due to blocking events over western Russia (Figure S5; Sousa et al., 2018).

Over the United Kingdom and northwestern France, the warming-trend contribution to the observed temperature is smaller (+0.2–0.3 °C) than the NAO+ (+0.2–0.6 °C) and Wave-7 contributions (+0.5–1.0 °C; compare Figure S3c with Figures 3b and 3c). Hence, there, the detrended atmospheric patterns played a bigger role. Finally, adding the warming-trend contribution to the temperature anomalies also strengthens differences, in agreement with the stronger negative difference in the Z300 west of Portugal and over Germany (Figures 3d and S4b).

The precipitation differences (Figures 4d and 4h) do not seem to be sensitive to the addition of the trend (compare Figures 4d and 4h with Figures S4c and S4f). Therefore, they might be due to local nonlinear processes (possibly related with orography) or to a missing pattern: Bladé et al. (2012) found weaker correlation between the summer NAO and precipitations in the Mediterranean region.

5. Summary and Conclusion

We investigated possible drivers of summer 2018 European contrasted weather. The extraordinary combination of a record high NAO and a strong Rossby Wave-7 pattern led to concomitant heat and precipitation events over Europe during a 3-week period starting on 21 June. Over the whole season, the combination of a persistent NAO+, the warming trend and, to a lesser extent, the Wave-7 explained most of the seasonal anomalies observed. This 3-week period was chosen for exhibiting strong anomalies characteristic of the seasonal mean, but we note that other patterns and events also occurred within this season. Therefore, this study does not aim to explain all the local or synoptic events occurring during summer 2018, such as the August heat waves over Iberia and Germany (NOAA, 2018; Pfleiderer et al., 2019), but rather the seasonal-mean European summer 2018 weather.

Contrary to the July 1976 heat wave over northwestern Europe that was due to blocking events (Green, 1977), the late June to mid-July 2018 heat wave is due to the combination of a record high NAO+ (Figures 1b and S2) and a strong Wave-7 (Figure 1c) over the NAE (see also Figure S5). This combination explains 80–100% of the observed anomalies over the United Kingdom, northwestern France, and Belgium. Over the rest of western Eurasia, these two patterns reproduce the observed anomalies with a less-than-1 °C error to the exception of Scandinavia and western Russia. There, the strong differences with the observed anomalies could be due to a combination of different factors such as limitations of the linear regression analysis, the nonstationarity of the NAO pattern (Baker et al., 2019; Bladé et al., 2012), the warming trend, other atmospheric circulation patterns, or local nonlinear processes (in relation with orography or soil-moisture feedback). Some studies

(e.g., Fischer, 2014; Miralles et al., 2014) have highlighted the importance of soil-moisture feedback in maintaining and strengthening heat waves. The NAO+ conditions since April–May 2018 (not shown) could have been responsible for the drier than average weather recorded over Europe over the same period (Toreti et al., 2019) and participated in the local increase in the temperature in JJA (not shown).

At the seasonal timescale, the Wave-7 contribution is very weak and the observed anomalies are mostly due to the combination of the strong NAO+ and the warming trend. This is consistent with the synoptic nature of the Wave-7 and also implies that strong seasonal impacts might not be expected from the Wave-7, despite strong synoptic impacts. On the contrary, strong persistent NAO+ can induce extreme weather conditions (flooding and heat waves) over western Eurasia both at synoptic and seasonal timescales. In addition, in late July to early August 2017, a strong NAO− was associated to the Lucifer heat wave over southeastern Europe, meaning that both phases are linked to extremely warm weather over different parts of Europe in summer (Kew et al., 2019). This clearly shows that persistent strong summer NAO can be considered as a driver of heat waves as well as blocking events (e.g., Drouard & Woollings, 2018; Röthlisberger & Martius, 2019; Schaller et al., 2018; Schneidereit et al., 2012; Sousa et al., 2018) or the Wave-7 (Kornhuber et al., 2019).

Several studies (e.g., Schaller et al., 2018; Sousa et al., 2017, 2018) showed that blocking impacts both 2-m temperature and precipitation and can induce heat waves in summer. Interestingly, during the 3-week period, no blocks were detected over Eurasia or the North Atlantic by the 2-D reversal method from Masato et al. (2013; Figure S5). Over JJA, a few blocks occurred over western Russia and could be responsible for the small temperature differences seen in Figure 3d. Overall, the blocking contribution to summer 2018 European weather appears limited. Note, though, that a range of types of blocks/anticyclones is possible, not necessarily detected by this method, and that these can have distinct regional impacts (Sousa et al., 2018).

Despite the combination of these two patterns, summer 2018 would not have been such a warm season without anthropogenic climate change, in agreement with Vogel et al. (2019). Indeed, over Scandinavia and Russia, the strong positive warming-trend contribution (+2.2 °C) reversed the negative NAO+ and Wave-7 contributions (−0.5–0 °C), inducing positive temperature anomalies where negative anomalies were expected. Elsewhere, the warming trend strengthens the positive NAO+ and Wave-7 contributions to the 2-m temperature anomalies.

Finally, the persistence of the NAO appears to be critical for extreme weather over Europe in summer. Spring sea surface temperature anomalies have been shown to be a potential driver of the summer NAO (Baker et al., 2019), which could allow for a possible prediction of such contrasted weather over Europe.

Acknowledgments
The authors would like to thank two anonymous reviewers for their constructive comments. Marie Drouard was funded by the NERC Grant NE/N01815X/1 and Kai Kornhuber by the NERC and NCAS Grants NE/N018001/1 and NE/P006779/1. All the data used in this paper were downloaded from the NOAA website (https://www.esrl.noaa.gov/psd/data/gridded/data.ncep.reanalysis.html).

References

Baker, H., Woollings, T., Forest, C., & Allen, M. (2019). The linear sensitivity of the North Atlantic Oscillation and eddy-driven jet to ssts. *Journal of Climate*, *32*, 6491–6511.

Bladé, I., Liebmann, B., Fortuny, D., & van Oldenborgh, G. J. (2012). Observed and simulated impacts of the summer NAO in Europe: implications for projected drying in the mediterranean region. *Climate dynamics*, *39*, 709–727.

Cattiaux, J., Vautard, R., Cassou, C., Yiou, P., Masson-Delmotte, V., & Codron, F. (2010). Winter 2010 in Europe: A cold extreme in a warming climate. *Geophysical Research Letters*, *37*, L20704. https://doi.org/10.1029/2010GL044613

Dong, B., Sutton, R. T., Woollings, T., & Hodges, K. (2013). Variability of the North Atlantic summer storm track: Mechanisms and impacts on European climate. *Environmental Research Letters*, *8*, 034037.

Drouard, M., & Woollings, T. (2018). Contrasting mechanisms of summer blocking over western Eurasia. *Geophysical Research Letters*, *45*, 12,040–12,048. https://doi.org/10.1029/2018GL079894

Feldstein, S. B. (2007). The dynamics of the North Atlantic Oscillation during the summer season. *Quarterly Journal of the Royal Meteorological Society*, *133*(627), 1509–1518.

Fischer, E. M. (2014). Climate science: Autopsy of two mega-heatwaves. *Nature Geoscience*, *7*, 332.

Folland, C. K., Knight, J., Linderholm, H. W., Fereday, D., Ineson, S., & Hurrell, J. W. (2009). The summer North Atlantic Oscillation: Past, present, and future. *Journal of Climate*, *22*, 1082–1103.

Green, J. (1977). The weather during July 1976: Some dynamical considerations of the drought. *Weather*, *32*(4), 120–126.

Hurrell, J. W., Kushnir, Y., Ottersen, G., & Visbeck, M. (2003). An overview of the North Atlantic Oscillation, *The North Atlantic Oscillation: Climatic significance and environmental Impact* (pp. 1–36). Washington, DC: Geophysical Monograph-American Geophysical Union.

Kalnay, E., Kanamitsu, M., Kistler, R., Collins, W., Deaven, D., Gandin, L., et al. (1996). The NCEP/NCAR 40-year reanalysis project. *Bulletin of the American meteorological Society*, *77*, 437–472.

Kew, S. F., Philip, S. Y., Jan van Oldenborgh, G., van der Schrier, G., Otto, F. E., & Vautard, R. (2019). The exceptional summer heat wave in southern Europe 2017. *Bulletin of the American Meteorological Society*, *100*, S49–S53.

Kornhuber, K., Osprey, S., Coumou, D., Petri, S., Petoukhov, V., Rahmstorf, S., & Gray, L. (2019). Extreme weather events in early summer 2018 connected by a recurrent hemispheric Wave-7 pattern. *Environmental Research Letters*, *14*, 054002.

Masato, G., Hoskins, B. J., & Woollings, T. (2013). Winter and summer Northern Hemisphere blocking in CMIP5 models. *Journal of Climate*, *26*, 7044–7059.

Met Office (2018). Summer 2018. https://www.metoffice.gov.uk/binaries/content/assets/metofficegovuk/pdf/weather/learn-about/uk-past-events/interesting/2018/summer-2018---met-office.pdf [Online]

Météo France (2018). Bilan climatique de l'été 2018. http://www.meteofrance.fr/climat-passe-et-futur/bilans-climatiques/bilan-2018/bilan-climatique-de-l-ete-2018 [Online]

Miralles, D. G., Teuling, A. J., Van Heerwaarden, C. C., & De Arellano, J. V.-G. (2014). Mega-heatwave temperatures due to combined soil desiccation and atmospheric heat accumulation. *Nature Geoscience*, *7*, 345.

NOAA (2018). Global climate report—2018. https://www.ncdc.noaa.gov/sotc/352global/2018 [Online]

NOAA (2018). Global climate report—August 2018. https://www.ncdc.noaa.gov/sotc/global/201808 [Online]

Pfleiderer, P., Schleussner, C.-F., Kornhuber, K., & Coumou, D. (2019). Summer weather becomes more persistent in a 2 °C world. *Nature Climate Change*, *9*, 1–6.

Röthlisberger, M., & Martius, O. (2019). Quantifying the local effect of northern hemisphere atmospheric blocks on the persistence of summer hot and dry spells. *Geophysical Research Letters*, *46*, 10,101–10,111. https://doi.org/10.1029/2019GL083745

Schaller, N., Sillmann, J., Anstey, J., Fischer, E., Grams, C., & Russo, S. (2018). Influence of blocking on northern European and western Russian heatwaves in large climate model ensembles. *Environmental Research Letters*, *13*(5), 054015.

Schneidereit, A., Schubert, S., Vargin, P., Lunkeit, F., Zhu, X., Peters, D. H., & Fraedrich, K. (2012). Large-scale flow and the long-lasting blocking high over Russia: Summer 2010. *Monthly Weather Review*, *140*, 2967–2981.

Sousa, P. M., Trigo, R. M., Barriopedro, D., Soares, P. M., Ramos, A. M., & Liberato, M. L. (2017). Responses of European precipitation distributions and regimes to different blocking locations. *Climate Dynamics*, *48*(3-4), 1141–1160.

Sousa, P. M., Trigo, R. M., Barriopedro, D., Soares, P. M., & Santos, J. A (2018). European temperature responses to blocking and ridge regional patterns. *Climate Dynamics*, *50*, 457–477.

Toreti, A., Belward, A., Perez-Dominguez, I., Naumann, G., Luterbacher, J., Cronie, O., et al. (2019). The exceptional 2018 European water seesaw calls for action on adaptation. *Earth's Future*, *7*, 652–663. https://doi.org/10.1029/2019EF001170

van Oldenborgh, G. J., Drijfhout, S., Van Ulden, A., Haarsma, R., Sterl, A., Severijns, C., et al. (2009). Western Europe is warming much faster than expected. *Climate of the Past*, *5*(1), 1–12.

Vogel, M., Zscheischler, J., Wartenburger, R., Dee, D., & Seneviratne, S. (2019). Concurrent 2018 hot extremes across northern hemisphere due to human-induced climate change. *Earth's Future*, *7*, 692–703. https://doi.org/10.1029/2019EF001189

World Weather Attribution Project (2018). Heatwave in northern Europe, summer 2018. https://www.worldweatherattribution.org/attribution-of-the-2018-heat-in-northern-europe/ [Online]